



Universiteit
Leiden
The Netherlands

Integrating palaeoproteomics into the zooarchaeological analysis of Palaeolithic bone assemblages

Sinet-Mathiot, V.

Citation

Sinet-Mathiot, V. (2023, March 23). *Integrating palaeoproteomics into the zooarchaeological analysis of Palaeolithic bone assemblages*. Retrieved from <https://hdl.handle.net/1887/3577205>

Version: Publisher's Version

License: [Licence agreement concerning inclusion of doctoral thesis in the Institutional Repository of the University of Leiden](#)

Downloaded from: <https://hdl.handle.net/1887/3577205>

Note: To cite this publication please use the final published version (if applicable).

Chapter Two

Combining ZooMS and zooarchaeology to study Late Pleistocene hominin behaviour at Fumane (Italy)

Virginie Sinet-Mathiot¹, Geoff M. Smith¹, Matteo Romandini^{2,3}, Arndt Wilcke⁴, Marco Peresani³, Jean-Jacques Hublin¹, Frido Welker^{1,5}

¹ Department of Human Evolution, Max Planck Institute for Evolutionary Anthropology, Leipzig, Germany.

² University of Bologna, Department of Cultural Heritage, Ravenna, Italy.

³ University of Ferrara, Department of Humanities, Section of Prehistory and Anthropology, Ferrara, Italy.

⁴ Fraunhofer Institute for Cell Therapy and Immunology, Leipzig, Germany

⁵ Evolutionary Genomics Section, Globe Institute, University of Copenhagen, Copenhagen, Denmark.

Published in *Scientific Reports*, 2019, volume 9, issue 12350.

<https://doi.org/10.1038/s41598-019-48706-z>

Abstract

Collagen type I fingerprinting (ZooMS) has recently been used to provide either palaeoenvironmental data or to identify additional hominin specimens in pleistocene contexts, where faunal assemblages are normally highly fragmented. However, its potential to elucidate hominin subsistence behaviour has been unexplored. Here, ZooMS and zooarchaeology have been employed in a complementary approach to investigate bone assemblages from final Mousterian and Uluzzian contexts at Fumane cave (Italy). Both approaches produced analogous species composition, but differ significantly in species abundance, particularly highlighted by a six fold-increase in the quantity of *Bos/Bison* remains in the molecularly identified component. Traditional zooarchaeological methods would therefore underestimate the proportion of *Bos/Bison* in these levels to a considerable extent. We suggest that this difference is potentially due to percussion-based carcass fragmentation of large *Bos/Bison* bone diaphyses. Finally, our data demonstrates high variability in species assignment to body size classes based on bone cortical thickness and fragment size. Thus, combining biomolecular and traditional zooarchaeological methods allows us to refine our understanding of bone assemblage composition associated with hominin occupation at Fumane.

Introduction

Zooarchaeological analyses use faunal remains to address archaeological questions. This provides a wealth of information on local and regional palaeoenvironments, the timing of hominin occupation, and interactions with other species¹⁻⁵. Most specifically, such studies have been used to reconstruct hominin diet and subsistence patterns. However, faunal remains are often highly fragmented by taphonomic, including anthropogenic processes, precluding any type of taxonomic identification for most specimens. The non-identifiable component of Pleistocene bone assemblages frequently incorporates 60–70% of the excavated assemblage^{6,7}. This leads to an extensive taxonomically uninformative proportion of bone assemblages, which could represent a source of bias in zooarchaeological studies of hominin subsistence behaviour.

Bone fragmentation can also provide a wealth of detail about site formation and depositional processes, but also more specifically about butchery practices and subsistence patterns. The species body part representation and the occurrence and location of cut-marks, percussion traces and bone breakage patterns can illustrate specific transport decisions by human groups⁸⁻¹⁰. However, large portions of bone assemblages remain taxonomically unidentifiable, and in the best cases can only be attributed to body size classes. Patterns of human subsistence behaviour are therefore often reliant on a relatively small proportion of morphologically identifiable remains. To provide a more comprehensive picture of human subsistence behaviour at a site requires the synthesis and analysis of comparable taxonomic

and taphonomic data from both identifiable and unidentifiable fraction of Pleistocene faunal assemblages.

With the advancement of biomolecular studies in the past 20 years, different methods have been developed in order to aid the identification and the analysis of biological markers preserved in unidentifiable bone fragments. First, ancient DNA metabarcoding of bone samples has been employed to study the taxonomic composition of hundreds or thousands of bone samples simultaneously^{11–13}. Second, various approaches involving ancient DNA sequencing have allowed the identification of vertebrate DNA directly from Pleistocene soil and sediment samples^{14–17}. Both approaches provide qualitative insights into species composition but, currently, little resolution in terms of quantitative aspects¹¹. In addition, all genetic and genomic approaches rely on ancient DNA survival, a biomolecule prone to fragmentation in comparison to other biomolecules, such as proteins^{18–20}. Therefore, proteomic approaches, in particular collagen type I peptide mass fingerprinting through Zooarchaeology by Mass Spectrometry analysis (ZooMS²¹), have been suggested as a biomolecular alternative to study the taxonomic composition of the unidentifiable component of Pleistocene bone assemblages. Proteins such as collagen type I are phylogenetically informative, easily accessible, and survive beyond the temporal range of ancient DNA^{22–24}.

ZooMS is a proteomic approach that allows taxonomic identification based on protein amino acid sequence variation through peptide mass fingerprinting²¹. This method is commonly performed on individual bone specimens in a targeted manner (for example on bone tools, particular taxonomic groups, or for radiocarbon or isotopic studies^{25–28}) and thereby provides quantitative datasets potentially comparable with traditional zooarchaeological studies. ZooMS can add additional information on hominin behaviour in relation to faunal carcass processing and selection^{29,30}, but this potential has not been explored. Nevertheless, previous studies have demonstrated that ZooMS is a robust tool that provides a high identification success rate (>95%) in the European Late Pleistocene. Initial taxonomic identifications through ZooMS have allowed the recovery of additional hominin specimens^{30–33}. Bone specimens individually identified through ZooMS can be utilised in subsequent ancient DNA, isotopic, and radiocarbon dating analysis^{34–37}. Finally, peptide mass fingerprints of collagen type I provide specimen-specific information of molecular diagenesis, allowing insights into spatial and temporal biomolecular preservation within a site^{38–40}.

In previous studies, ZooMS- and morphologically-identified components from the same layers are comparable in terms of species composition and abundance (Fig. 1). On some sites, the application of this method has allowed for the identification of species previously unconfirmed through traditional morphological analysis^{29,30,38,41}. However, no ZooMS studies have investigated the relationship between faunal composition and bone fragmentation and, in turn, whether this is related to specific hominin behaviour at a site. In this study, 684 bone

specimens across the Middle to Upper Palaeolithic transition (MUPT) corresponding to layers A6 to A2 at Fumane (Italy), have been analysed, with a focus on the Final Mousterian layer A4 (previously attributed to the Uluzzian: see ref.⁴²) and the Uluzzian layer A3^{43–46}.

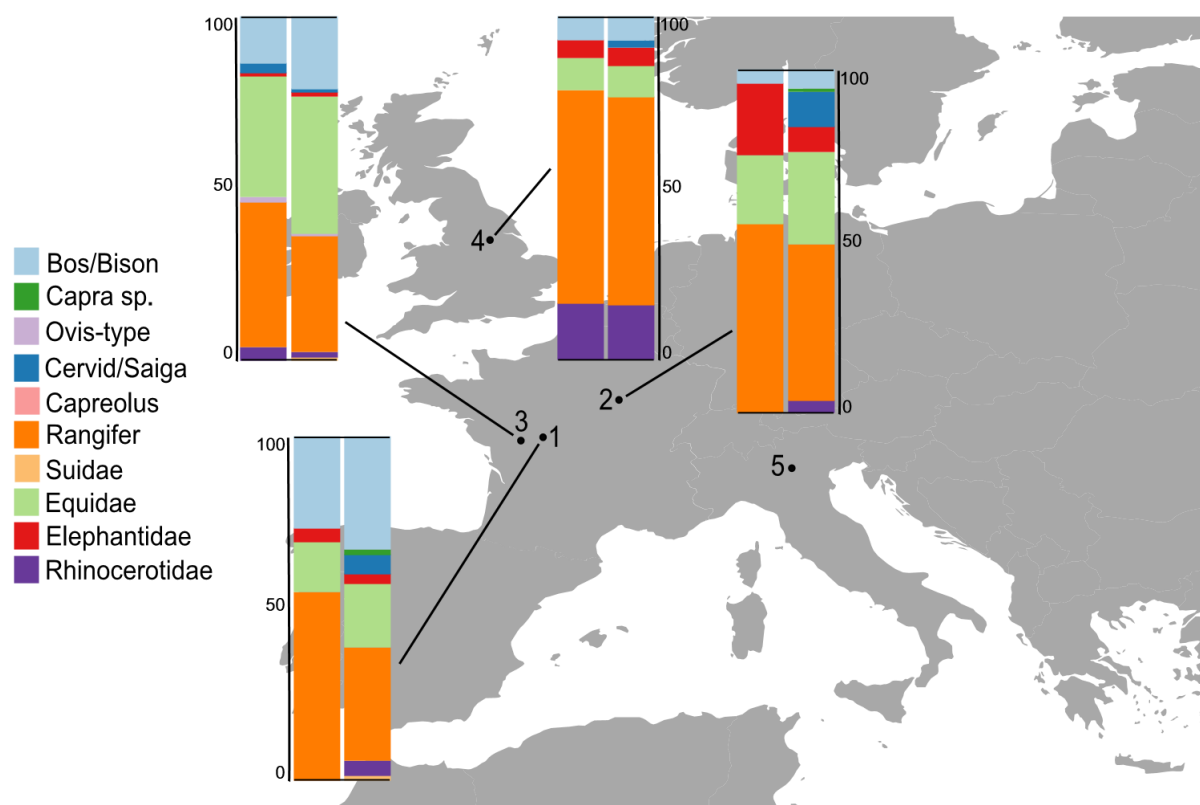


Figure 1. Site location of Fumane and other published, non-targeted ZooMS studies with zooarchaeological data available for the same archaeological layers. For each site the barplot indicates the percentage of number of identified specimens (%NISP) of herbivores for the morphologically identified (left) and the ZooMS component (right). 1: Les Cottés (France)²⁹ (ZooMS: N = 70, Morph: N = 75), 2: Grotte du Renne (France)³⁰ (ZooMS: N = 108, Morph: N = 100), 3: Quinçay (France)³⁸ (ZooMS: N = 412, Morph: N = 213), 4: Pin Hole Cave (UK)⁴¹ (ZooMS: N = 72, Morph: N = 78), 5: Fumane (Italy; this study see Fig. 3). Further details are provided in Supplementary Table S1.

Methods

Fumane

Fumane cave is located at the bottom of the Venetian Pre-Alps within the Western Monti Lessini in North of Italy (Fig. 1). The site has been known since the late 19th century, and was first excavated in 1964 by the Natural History Museum of Verona. The current excavations are led by a team from the University of Ferrara, and the faunal assemblage from these excavations were sampled and analysed to form the basis of this study.

The cave is part of a karst system composed of several cavities which has permitted the accumulation of a sedimentary sequence including Mousterian, Uluzzian and Aurignacian

cultural complexes^{45–49}. Human occupation at Fumane is attested by numerous faunal remains, lithics artefacts and combustion features. The site also offers unusual finds such as ornamental objects, painted stones, and evidence for the intentional removal of feathers from birds^{50–53}. Various studies have presented radiocarbon dates, Uranium-Thorium dates, and electron spin resonance (ESR) combined dates, that provide a clear chronological framework for the entire stratigraphy^{47,54}, in addition to palaeoecological contexts⁵⁵. Within this framework, layers A4 and A3 date between 41.3 and 39.1 ka (Table 1)^{56,57}.

The bone assemblages from Fumane are highly fragmented across the stratigraphy^{43,58–60}. For example, for layers A3 and A4 about 3% of the assemblage (1,188 out of 36,944 bone remains including dental remains) can be securely identified based on morphological characteristics. For these 2 layers, the faunal spectrum based on the morphologically identifiable bones includes various ungulates, carnivores and birds, which together indicate a closed wooded environment indicative of temperate to cool climatic conditions^{43,59}. The differences in faunal composition between layers A3 and A4 are relatively minor, and they occur in the abundance of the dominant species (Table 1).

Layer	Cultural attribution	Approximate age	Dominant faunal components (%NISP)
D3	Aurignacian		Ibex (<i>Capra ibex</i> , 43.0%)
D6	Aurignacian		Ibex (<i>Capra ibex</i> , 35.5%)
A1	Protoaurignacian		Ibex (<i>Capra ibex</i> , 43.9%), red deer (<i>Cervus elaphus</i> , 18.4%)
A2-A2R	Protoaurignacian	41–38 ka cal BP	Ibex (<i>Capra ibex</i> , 49.5%), red deer (<i>Cervus elaphus</i> , 18.8%)
A3	Uluzzian	44–42 ka cal BP	Red deer (<i>Cervus elaphus</i> , 29.5%), ibex (<i>Capra ibex</i> , 20.3%)
A4	Final Mousterian (Levallois)	44–42 ka cal BP	Red deer (<i>Cervus elaphus</i> , 39.3%), ibex (<i>Capra ibex</i> , 20.3%)
A5-A6	Mousterian (Levallois)	45–44 ka cal BP	Red deer (<i>Cervus elaphus</i> , 70.3%), roe deer (<i>Capreolus capreolus</i> , 11.7%)
A7	(-)		No human presence
A9	Mousterian (discoidal)	>47.6 ka cal BP	Red deer (<i>Cervus elaphus</i> , 39.3%), roe deer (<i>Capreolus capreolus</i> , 22.3%)
A10	Mousterian (Levallois/discoidal)	>47.6 ka cal BP	Roe deer (<i>Capreolus capreolus</i> , 43.8%), red deer (<i>Cervus elaphus</i> , 29.5%)
A11	Mousterian (Levallois)	>47.6 ka cal BP	Roe deer (<i>Capreolus capreolus</i> , 39.5%), red deer (<i>Cervus elaphus</i> , 32.3%)

Table 1. Fumane stratigraphy, chronological age, and faunal composition based on morphologically identifiable bone specimens. Reference data on chronology taken from^{44,47,56}. Reference data for zooarchaeological analysis taken from^{43,51,58–60,115}. Note that layer A4 is now attributed to the Final Mousterian. See discussion in⁴².

Zooarchaeological analysis

In the zooarchaeological analysis of the bone assemblages from Fumane, all the remains have been counted and grouped by size (0–1 cm, 1–2 cm, 2–3 cm, 3–4 cm, 4–5 cm, >5 cm). Burned and calcined bones were separated from the unburned specimens. All bone specimens were also grouped by body size class (large, medium-large, medium, medium-small, and small) based on bone cortical thickness and fragment size.

Taxonomic and skeletal identification was based on two reference collections. The first is stored at Lazio Museum Pole at the National Prehistoric Ethnographic Museum “Luigi Pigorini” in the Bioarchaeology Section in Rome, while the second is in the Prehistoric and Anthropological Sciences Section at the University of Ferrara. Microscopic analyses of the bone surfaces were carried out using portable low-magnification lenses (10–20X) and Leica S6D Green Ough stereomicroscopes with 0.75–70X magnification range. In specific cases, observation was also carried out using scanning electron microscopy (SEM).

In order to determine the nature of surface bone alterations, and to distinguish hominin from animal traces, trampling abrasion, and modern mechanical modifications produced by excavation tools, reference was made to the well-established taphonomic literature^{61–68}. The degree of combustion was evaluated employing the methodology developed by Stiner *et al.*⁶⁹. All faunal specimens were analysed, regardless of their taxonomic identifiability by one of the authors (M.R.) using traditional morphological observation. For our study, species abundance was assessed using the number of identified specimens (NISP)⁷⁰, as minimum number of skeletal element (MNE) and minimum number of individuals (MNI) cannot be compared quantitatively with ZooMS data, which is inherently a NISP count. The percentage of the number of identified specimens have been calculated based on the taxonomically identified faunal specimens. Finally, bone fragmentation indices were calculated to evaluate the skeletal representation of the different animals and the skeletal survival rate^{61,62,67}.

ZooMS

684 morphologically unidentifiable bone and dental (dentine) specimens have been randomly sampled across levels A6 to A2 excavated in the same squares in the western area of the cave entrance (Supplementary Table S2). The majority of these bone specimens (73%) derive from the two layers A3 and A4. All selected specimens were recorded as individual specimens during excavation. For bone specimens, selection was based on the presence of cortical bone surface and a length of at least 2 cm. Dental specimens comprise a minor proportion of the analyzed samples (n = 8, 1.2%) and were excluded from surface modification analysis. For layers A3 and A4, our sampling covered the same spatial distribution (Supplementary Table S2). The maximum length of the bone specimens was measured individually with a digital calliper. ZooMS-identified bone specimens had previously been

analysed morphologically and various taphonomic attributes recorded, allowing for the comparison of surface modification frequencies related to taphonomic and anthropogenic processes present in both components of the bone assemblages.

ZooMS extraction methods followed protocols outlined in detail elsewhere³⁰. In short, soluble collagen is first extracted from small bone samples (<20 mg) by incubation in 100 μ L 50 mM ammonium-bicarbonate buffer at 65 °C for 1 hour. Half of this is digested using trypsin (0.5 μ g/ μ L, Promega) overnight, acidified to pH < 1 using TFA (10% TFA), and cleaned on C18 ZipTips (Thermo Scientific). Hereafter, this is referred to as the “AmBic” extraction method⁴⁰. Digested peptides are subsequently spotted in triplicate on a MALDI Bruker plate (MTP AnchorChip 384) with the addition of α -Cyano-4-hydroxycinnamic acid (CHCA) matrix. MALDI-TOF MS analysis was conducted at the University of York on an Ultraflex mass spectrometer (Bruker) in the mass-to-charge range 900–4000 m/z. MALDI-TOF stands for Matrix-assisted Laser-Desorption/Ionization, a method to ionize molecules, and is based on the co-crystallization of the matrix and an analyte, i.e. the substance to be analysed, in this case a bone proteome digested with trypsin. Analyte molecules are incorporated into the matrix while crystallization takes place. Subsequent laser impulses result in the detachment of crystalline particles into the vacuum of the mass spectrometer. Based on their time-of-flight (TOF) to the spectrometer’s detector, the molecular mass(es) of the analyte can be determined. Triplicates were merged for each sample, and taxonomic identification proceeded through peptide marker mass identification in comparison to a published database containing peptide marker series for all medium-to larger sized mammalian genera in existence in Europe during the Pleistocene^{21,30}.

For 24 samples, the AmBic taxonomic identity based on soluble collagen was verified through subsequent demineralization of the sample in 0.6 M HCl, neutralization to pH 6–7, and protein solubilization again in 0.6 M ammonium-bicarbonate (hereafter the “HCl” extraction method)²¹. All subsequent steps for these 24 specimens were identical to the “AmBic” extraction method except that they were analysed at the MALDI-TOF MS facility at the Fraunhofer IZI in Leipzig, Germany, using an autoflex speed LRF MALDI-TOF (Bruker) in reflector mode, positive polarity, matrix suppression of 590 Da, and collected in the mass-to-charge range 800–4000 m/z.

Soluble collagen deamidation was calculated for selected peptides frequently observed in peptide fingerprints of collagen type I through published protocols^{71,72}. Glutamine deamidation has been suggested as an indicator of collagen preservation variability^{38,72}. Only slow-deamidating peptides have been observed to be frequently present in the Fumane spectra, and we hence limit our analyses to these peptides (P1105 and P1706). Deamidation ratios are presented on a scale from 0 (complete deamidation, all glutamines converted into glutamic acid) to 1 (no deamidation, all glutamines unmodified).

All analyses were conducted in R⁷³, and figures were produced using the package ggplot2⁷⁴.

Results

Our analysis resulted in successful ZooMS identifications for 97.8% of a total of 684 bone specimens, with nearly identical success rates across all sampled levels (Supplementary Table S2). Deamidation values for all bone specimens indicate a temporal cline towards more extensive diagenetic modification for older layers (Supplementary Fig. S1). Extraction blanks to monitor protein contamination in the lab were empty of collagen type I. Furthermore, HCl demineralization and MALDI-TOF-MS analysis of a randomly selected set of 24 *Bos/Bison* specimens after AmBic analysis resulted in identical taxonomic identifications for both AmBic and HCl extraction methods (Supplementary Fig. S2). Our results are therefore difficult to explain by (laboratory) protein contamination.

Species presence in A3 and A4 is consistent between the ZooMS- and morphology-components of both levels (Supplementary Table S3). Exceptions are the addition of *Elephantidae* and *Rhinocerotidae* through ZooMS analysis for layer A4 and the presence of several carnivore species in the morphology-component⁴³. This observation is similar to those made for previous untargeted ZooMS studies^{29,30,38}. There are no herbivore species identified morphologically that are not represented in the ZooMS-component.

In zooarchaeology, bone specimens are frequently categorised in body size classes when species identification is not possible based on morphological criteria. At Fumane, bone fragment size and cortical thickness has been used as a proxy for body size class assignments. ZooMS analysis of bone specimens with body size class (BSC) assignments reveals that such categorizations are highly variable. For example, we note the presence of *Caprinae* within the large body size class and bone fragments identified as *Elephantidae* and *Bos/Bison* assigned to the medium body size class (Fig. 2). Thus, using the Fumane dataset, we illustrate that attributing taxonomically unidentifiable components to body size class categories (large, medium-large, medium) remains a useful, but problematic, qualitative tool. Moreover, these attributions are not taxonomically reliable as bone fragment size and cortical thickness are dependent on numerous overlapping and interrelated biological and taphonomic factors. As such, these body size class categories may not accurately reflect overall species composition at a site.

In contrast to previous studies (Fig. 1), a large difference in the quantitative composition of the ZooMS-component and the morphologically-identified component have been observed for layers A3 and A4 (Fig. 3). As ZooMS analysis cannot be performed on burned bone it was important to have comparable datasets for both the morphological and ZooMS component. Therefore, we assessed the proportion of burned and unburned specimens by taxon in the

morphological component from A3 and A4 (Fig. 3). The species representation is similar for both burned and unburned portions.

Overall, species representation among layers A3 and A4 is driven by an almost 6-fold increase in the number of *Bos/Bison* specimens in the ZooMS-component (36%) compared to the morphology-component (6%) (Fig. 3), and counterbalanced by a relative decrease in the number of specimens attributed to *Capra* sp. Such a frequency difference in the presence of a particular species between the ZooMS- and morphology-components of the same archaeological layer has never been observed until now (Fig. 1). The remainder of this paper aims to explore potential causes of this compositional difference by focusing on the three main taxonomic components (*Capra* sp., Cervid/Saiga, and *Bos/Bison*) of the layers A3 and A4.

For these three species groups, the spatial distribution of the bone specimens is more restricted in the ZooMS component (Fig. 4). The studied bone fragments have nearly identical distributions of specimen length (Fig. 5a). Whilst *Bos/Bison* specimens (41.7 ± 16.9 mm) are longer than *Capra* sp. specimens (37.1 ± 16.0 mm) and Cervid/Saiga specimens (39.6 ± 15.0 mm), there is no significant difference in the overall distributions (Cervid/Saiga versus *Capra* sp.: t-test(0.7), df = 20, $p = 0.48$; Cervid/Saiga versus *Bos/Bison*: t-test(-1.1), df = 178, $p = 0.27$; *Capra* sp. versus *Bos/Bison*: t-test(-1.2), df = 22, $p = 0.23$). However, considering that bone specimens of over 2 cm in length have been selected for this study, the distribution might not be similar for the smallest, unstudied, size range (0–2 cm). Finally, there is no apparent difference in the spatial distribution of bone fragment size (Fig. 4d). Altogether, we therefore conclude that, assuming *Bos/Bison* individuals are generally larger than *Capra* sp. and Cervid/Saiga individuals, *Bos/Bison* bone elements have been subjected to a larger amount of fragmentation.

Bone length and P1105 deamidation, an indicator of molecular collagen type I preservation, display no significant relationship for any of the three species groups (Fig. 5b; Spearman rank correlation, $R_s = 0.09$ $p = 0.19$). All specimens from layers A3 and A4 display an identical distribution of P1105 deamidation (t-test(1.5), df = 420, $p = 0.14$) (Fig. 5c) and show no spatial differences in the amount of average deamidation per square in the area analyzed (Fig. 4c). However, Cervid/Saiga specimens have a deamidation distribution significantly different from that observed for *Capra* sp. and *Bos/Bison* specimens (Cervid/Saiga versus *Capra* sp.: t-test(-5.9), df = 21, $p = 6.4 \cdot 10^{-06}$; Cervid/Saiga versus *Bos/Bison*: t-test(-6.8), df = 171, $p = 1.4 \cdot 10^{-10}$), while *Capra* sp. and *Bos/Bison* specimens have similar distributions (t-test(0.9), df = 25, $p = 0.39$). This reveals that Cervid/Saiga specimens have undergone a different extent of molecular diagenesis, but not fragmentation, compared to bone specimens from the other ZooMS-identified species.

The frequency of bone surface modifications due to non-anthropogenic taphonomic processes (e.g., weathering, concretion, corrosion, mineral staining and root etching) is broadly similar

for all three species groups in both the ZooMS and morphology component, as is the presence of carnivore and/or rodent marks (Supplementary Tables S4, S5). Thus, non-anthropogenic bone surface modifications appear to have affected all three species groups to a similar extent. Similarly, increased levels of molecular damage for Cervid/Saiga specimens can only be explained by a mechanism unrelated to bone fragmentation processes, but this cannot explain the increase in *Bos/Bison* specimens in the ZooMS component.

Likewise, bone surface modifications resulting from anthropogenic processes are present to a similar extent in the ZooMS- and morphologically-identified components. In general, such bone surface modifications are recorded in comparable frequencies, but the frequencies for cut marks and impact points (or loading point)⁶⁷ are more distinct (Supplementary Table S4). It should be noted that frequencies differ between species to some extent, but generally not between the morphology- and ZooMS-components within the same species. For example, there seem to be fewer anthropogenic modifications of *Capra sp.* specimens compared to both Cervid/Saiga and *Bos/Bison* specimens (Supplementary Table S4). We note, however, high frequencies of percussion marks for *Bos/Bison* specimens in the ZooMS-component of both A3 (30%) and A4 (11%; Supplementary Table S4 and Fig. 6). Such marks are absent for *Bos/Bison* in the same layers (0% and 0%, respectively) in the morphology-component, mostly represented by bone epiphysis, but also by carpals, tarsals, and distal limb bones. This is in contrast to the ZooMS assemblages, which are mainly composed of long bone fragments (diaphysis) and ribs. Indeed, percussion marks on *Bos/Bison* specimens are exclusively present on long bone diaphyses in our ZooMS-identified sample set. These are bone elements subjected to more intense processing during butchering and bone marrow extraction^{4,8,75}. Moreover, these specific traces appear to occur at much lower frequencies in the Cervid/Saiga (2–4%) and *Capra sp.* (0–0%) specimen groups.

All these observations related to bone surface modifications are replicated when the analysed specimens are restricted to the same set of squares for both the ZooMS and morphology components of the faunal assemblage (Supplementary Table S2). Alongside the absence of spatial patterns in bone fragmentation (Fig. 4d) and molecular degradation (Fig. 4c), there is therefore also no apparent spatial patterning in occurrence and frequency of bone surface modifications.

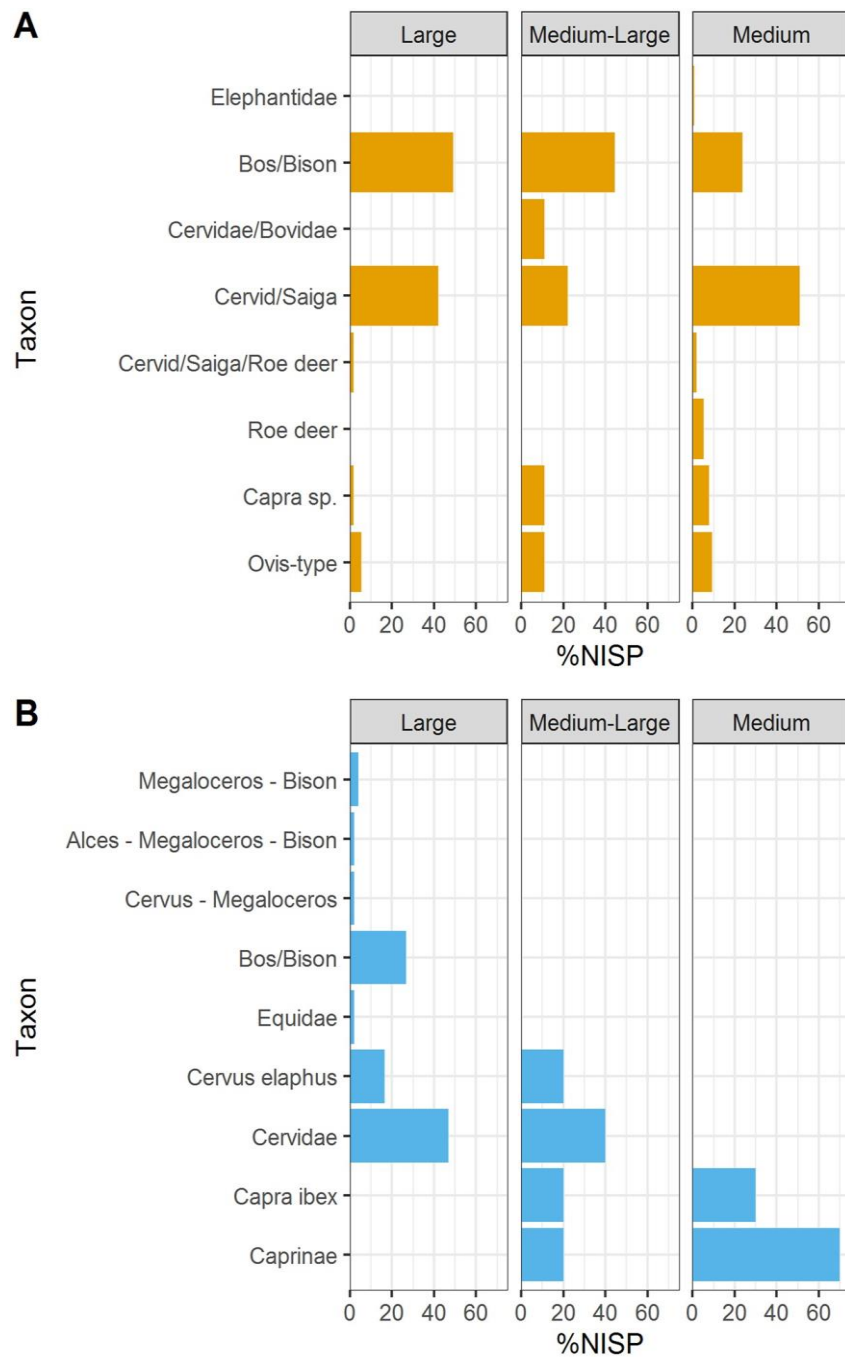


Figure 2. Barplot illustrating relative frequency (%NISP) for taxa identified using ZooMS (**A**) and morphology (**B**) in relation to their body size class attribution.

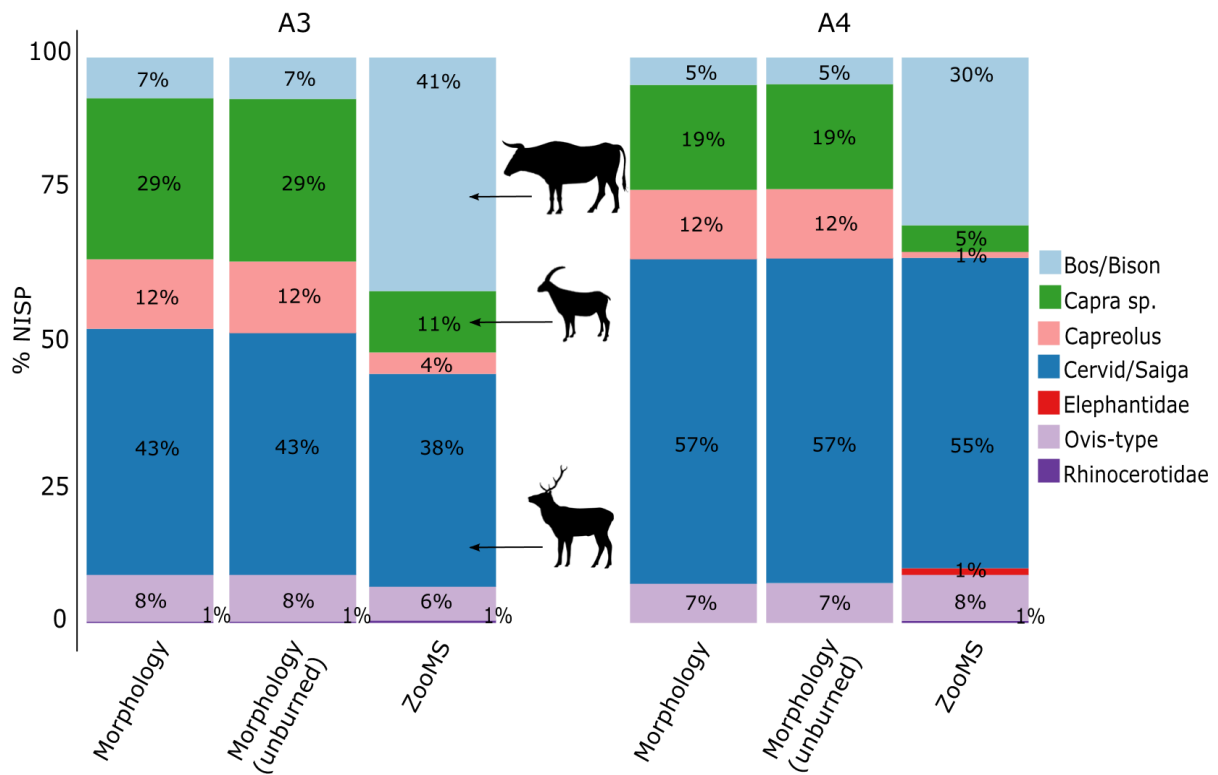


Figure 3. Barplot of %NISP of identified herbivores at Fumane. Morphology: this includes all specimens identified morphologically. Morphology (unburned): this includes specimens identified morphologically but excludes burned fragments (A3: 0.11% of burned specimens out of the morphology-identified assemblage (N = 453); (A4) 0.16% of burned bone fragments out of the morphological faunal assemblage (N = 681)). ZooMS: all specimens identified through ZooMS analysis (does not include burned fragments; see text for details). Colours are similar to Fig. 1. Data for the morphology-component derives from Tagliacozzo *et al.*⁴³. Animal silhouettes are not to scale and derive from phylopic.org.

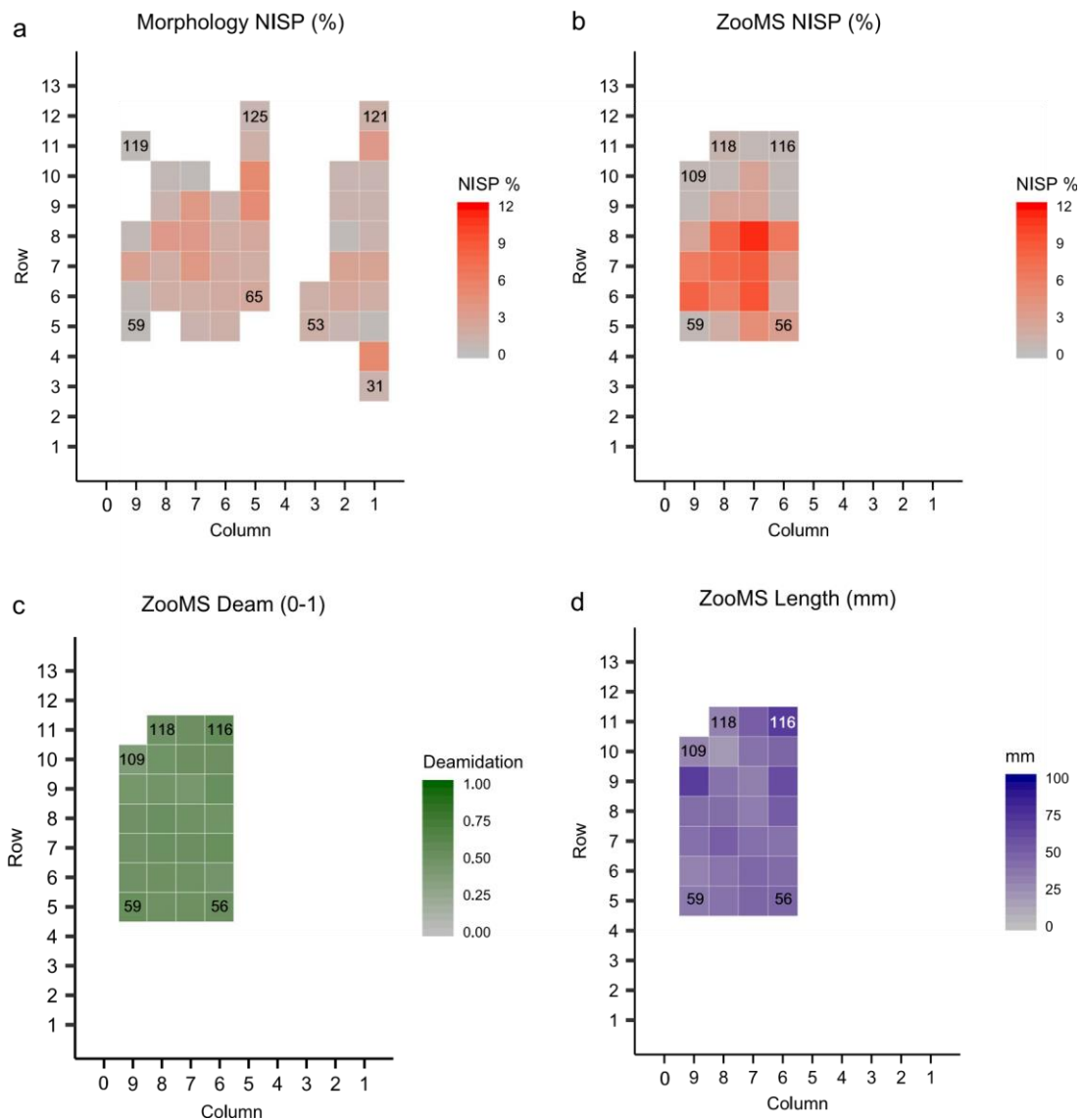


Figure 4. Spatial distribution maps of all bone specimens from the species groups Cervid/Saiga, *Capra* sp. and *Bos/Bison* from layers A3 and A4 at Fumane cave. **(a)** Distribution of %NISP of the three identified species for the morphology-component, over the sampled squares. **(b)** Distribution of %NISP of the three identified species for the ZooMS-component, over the sampled squares. **(c)** Average deamidation per square for the ZooMS component. **(d)** Average length (mm) per square for the ZooMS component. Squares are 1 × 1 meter, and the corresponding excavation numbers for each square can be obtained by joining the y-axis number and the x-axis number (for a detailed excavation plan, see⁵⁹). The numbers within the squares represent the square numbers from the excavation grid. For **a** and **b**, a %NISP of 12% would indicate that 12% of the NISP of the combined total of *Capra* sp., *Bos/Bison*, and Cervid/Saiga is derived from that square.

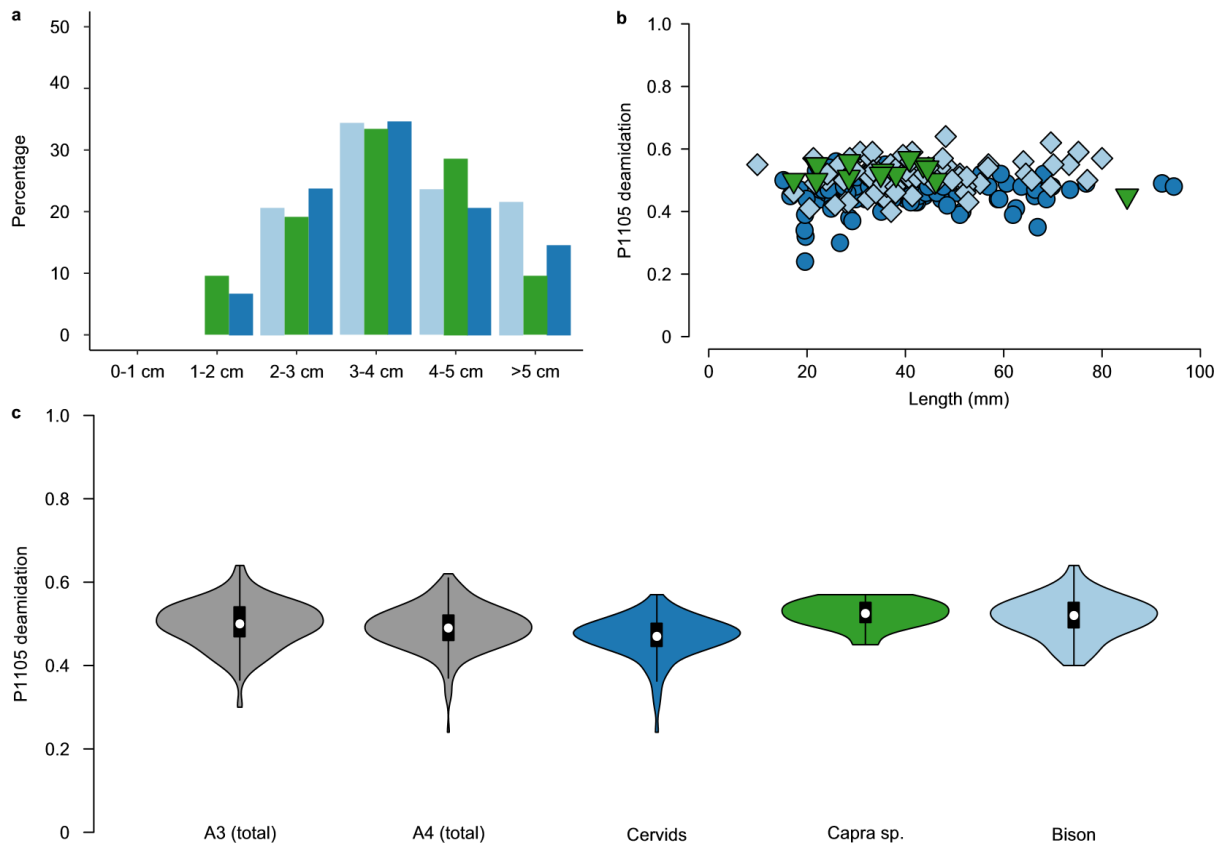


Figure 5. Taphonomic and molecular preservation of Cervid/Saiga, *Capra* sp., and *Bos/Bison* specimens. **(a)** Bone length distribution in mm. **(b)** Absence of a relationship between bone length (mm) and molecular diagenesis (P1105 deamidation). **(c)** Violin plots of P1105 deamidation. A3 and A4 include all specimens identified through ZooMS for these levels. Note that Cervid/Saiga is the dominant species group for both A3 and A4, significantly influencing the total violin plots for both levels displayed on the left. Only data for A3 and A4 are included for each panel. Colour legend is identical across panels as well as Figs. 1 and 3 (Cervid/Saiga: dark blue, *Capra* sp.: green and *Bos/Bison*: light blue).

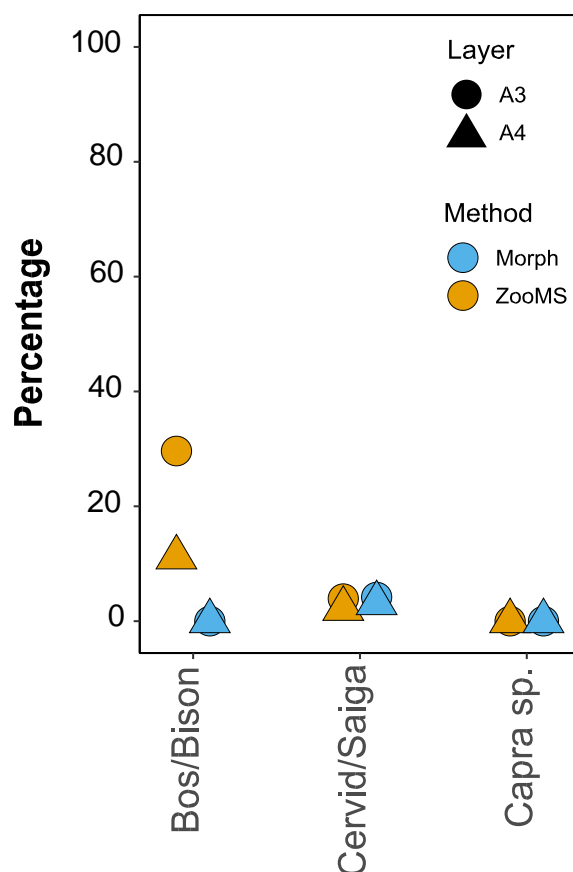


Figure 6. Percussion marks frequencies for the three main species groups within the morphology and the ZooMS-identified component in layers A3 and A4. Y-axis gives the percentage of occurrence (0–100) of percussion marks per specimen for the three major species groups (x-axis). Different point shapes indicate different layers (circle: A3; triangle: A4) whilst colour illustrates different identification method (blue: morphologically identified; gold: ZooMS). See Supplementary Table S4 for associated NISP numbers.

Discussion

Palaeoproteomics, including ZooMS, is a recent addition to the molecular toolkit available to explore past faunal communities^{21,29}, the phylogenetic relationships between those species^{20,22,76,77}, and hominin interactions with their immediate environment⁷⁸. ZooMS in particular has been adopted to survey the unidentifiable bone component of Palaeolithic sites in order to identify additional hominin remains^{30–33} and to explore the qualitative aspects of faunal assemblages. Archaeological complexes like the Uluzzian in Italy have been attributed to the transitional phase between the Middle and the Upper Palaeolithic marked by the diffusion of populations of anatomically and genetically modern hominins and the local extinction of Neanderthals^{46,79–82}. However, few hominin remains are directly attributable to the Uluzzian. Those that are available are associated with complicated debates on their taphonomic history^{83–85}, or cannot be reliably assigned to Neanderthals or modern hominins based on morphological characteristics because of their elevated degree of fragmentation or

the uncertain stratigraphic position^{86,87}. Although no additional hominin specimen attributable to the Uluzzian has been identified here, our dataset adds to a growing understanding of hominin interactions with the environment around the MUPT^{88–92}.

Alongside similar methods based on ancient DNA sequencing, ZooMS has the ability to provide quantitative data on the abundance of particular species. This quantitative aspect has not been explored up to now, however, partly because previous studies indicated little quantitative difference between morphology-identified and ZooMS-identified components of the same assemblage (Fig. 1). Here we have encountered an assemblage where the morphology- and ZooMS-identified components are relatively similar in terms of species composition but markedly different in quantitative aspects for two distinct archaeological layers at the same site. In particular, a 6-fold increase in *Bos/Bison* specimens in the ZooMS-component. This is counterbalanced by a 3-fold decrease in *Capra* sp. (Fig. 3). We observe no apparent spatial differences in bone fragmentation (Fig. 4d) or molecular diagenesis (Fig. 4c). However, we note that Cervid specimens are more deamidated than other bone specimens at the site. It is therefore possible that the enhanced deamidation of Cervids in A3 and A4 is the result of hominin behaviour, although we are unable, at present, to precisely define which kind of anthropogenic process might be responsible. Possibilities include boiling, low-temperature roasting, or fermentation, but a precise assessment requires the development of further molecular methods to identify and distinguish these different anthropogenic processes. Furthermore, slightly higher rates of Cervid collagen deamidation cannot explain the higher incidence of *Bos/Bison* specimens.

Bones fractured deliberately to extract marrow have been previously noted in both layers at Fumane⁴³. Compared to the morphologically identified assemblage, high frequencies of percussion marks on ZooMS-identified *Bos/Bison* specimens have been observed (Fig. 6). Therefore, the larger size of *Bos/Bison* elements and higher frequency of long bone diaphysis fragments and marrow fractures in the ZooMS-identified assemblage might explain the higher incidence of this species. Consequently, without the addition of the ZooMS dataset our interpretation of assemblage composition and human subsistence behaviour at Fumane would have been incomplete. The complementary ZooMS and zooarchaeological datasets from Fumane have provided a more comprehensive picture of assemblage composition and highlighted variation in the intensity and treatment of different prey sizes. This is exemplified by the increased fragmentation of *Bos/Bison* remains.

Palaeolithic faunal assemblages are often characterized by a high degree of fragmentation. This phenomenon can result from a number of natural taphonomic agents and processes^{67,93–102} but also due to intensive hominin carcass processing. Indeed, such patterns appear similar whether in the Lower^{98,101,103–106}, Middle^{2,107–111} or Upper Palaeolithic^{88,112}. Often, long bones and rib fragments represent, by far, the largest proportion of the unidentified component of

faunal assemblages^{109,113}. Similarly, these body regions represent high utility in terms of available resources (e.g., meat, marrow) and are thus frequently fragmented^{6-8,114}. This, undoubtedly, leads to a loss of taxonomic identification and hominin behavioural information, with behavioural interpretations based on a relatively small proportion of identifiable remains. The novel application of ZooMS to taxonomically unidentifiable specimens has the potential to provide a clearer picture of overall species composition at a site and can help to reduce analyst error, especially when faced with a large proportion of one species within the morphologically identified component.

Comparisons of the relative proportions of species within the morphological and ZooMS components provides complementary data about species abundance and environmental context at sites though these datasets have not, to date, been used to address broader zooarchaeological questions related to site use, assemblage formation, or hominin subsistence behaviour. The current study presents a first attempt to integrate complementary data sets from zooarchaeological and ZooMS-based analyses. Whilst the morphologically-identified assemblage may be dominated by a small number of species, sometimes a single species, this may not necessarily reflect true assemblage abundance. Body size class based on bone cortical thickness can provide a qualitative assessment of assemblage fragmentation. Comparative analysis at Fumane illustrates considerable variation between the ZooMS and morphological datasets when assigning bone fragments to specific body size classes based on fragment size and cortical bone thickness. Subsequent ZooMS analysis illustrates a scattering of species across and within these categories (e.g. *Elephantidae* in the medium size class, *Capra* sp. in the large size class) (Fig. 2). Body size class attributions should therefore be used with caution. Instead, molecular approaches like ZooMS can provide a more secure assignment of taxonomic identity and gives a more informative picture of species proportions, and associated bone surface modifications, within an assemblage.

Conclusion

Faunal remains from archaeological sites allow us to reconstruct how hominin populations adapted to changing climates and environments through the detailed study of patterns of hominin subsistence. Faunal analysis provides ecological information and also illustrates hominin behaviour associated with prey choice and carcass exploitation. High bone fragmentation rates, due to both natural and anthropogenic processes, result in low proportions of morphologically identifiable remains for many Palaeolithic faunal assemblages. Previous studies have relied solely on morphologically identifiable fauna, which can potentially exclude vast quantities of specimens and archaeologically valuable data. Through the biomolecular analysis of a large number of unidentifiable bone fragments, we have observed a significant quantitative difference in the ZooMS faunal spectrum compared to the

morphologically identifiable portion within the same assemblage. This is most evident as a 6-fold increase in the number of *Bos/Bison* specimens in the morphologically unidentifiable fragments; this is possibly due to the size of *Bos/Bison* bone elements, their processing during food procurement, and differences in bone elements identified through molecular and morphological methods of taxonomic identification. We also demonstrate that assigning bone fragments to body size classes based on bone cortical thickness and fragment size is an unreliable predictor of taxonomic identity, and these categorizations should therefore be used cautiously in behavioural interpretations of assemblage formation. We have thereby demonstrated that combining molecular and traditional zooarchaeological analysis can provide additional complementary insights into Pleistocene faunal assemblages and hominin subsistence behaviour.

References

1. Smith, G. M. Neanderthal megafaunal exploitation in Western Europe and its dietary implications: a contextual reassessment of La Cotte de St Brelade (Jersey). *J. Hum. Evol.* **78**, 181–201 (2015).
2. Gaudzinski-Windheuser, S., Kindler, L., Pop, E., Roebroeks, W. & Smith, G. The Eemian Interglacial lake-landscape at NeumarkNord (Germany) and its potential for our knowledge of hominin subsistence strategies. *Quat. Int.* **331**, 31–38 (2014).
3. Gaudzinski, S. & Roebroeks, W. Adults only. Reindeer hunting at the middle palaeolithic site salzgitter lebenstedt, northern Germany. *J. Hum. Evol.* **38**, 497–521 (2000).
4. Niven, L. *et al.* Neandertal mobility and large-game hunting: the exploitation of reindeer during the Quina Mousterian at ChezPinaud Jonzac (Charente-Maritime, France). *J. Hum. Evol.* **63**, 624–635 (2012).
5. Ruth, B. & Marco, P. Others. Human-bird interactions in Prehistory. Session B8, XVII UISPP Congress. *Quat. Int.* **421**, 1–5 (2016).
6. Morin, E., Ready, E., Boileau, A., Beauval, C. & Coumont, M.-P. Problems of Identification and Quantification in Archaeozoological Analysis, Part I: Insights from a Blind Test. *Journal of Archaeological Method and Theory* **24**, 886–937 (2017).
7. Morin, E., Ready, E., Boileau, A., Beauval, C. & Coumont, M.-P. Problems of Identification and Quantification in Archaeozoological Analysis, Part II: Presentation of an Alternative Counting Method. *Journal of Archaeological Method and Theory* **24**, 938–973 (2017).
8. Morin, E. Fat composition and Nunamiut decision-making: a new look at the marrow and bone grease indices. *J. Archaeol. Sci.* **34**, 69–82 (2007).
9. Jones, K. T. & Metcalfe, D. Bare bones archaeology: Bone marrow indices and efficiency. *J. Archaeol. Sci.* **15**, 415–423 (1988).
10. Metcalfe, D. & Jones, K. T. A Reconsideration of Animal Body-Part Utility Indices. *Am. Antiq.* **53**, 486–504 (1988).
11. Grealy, A. C. *et al.* A critical evaluation of how ancient DNA bulk bone metabarcoding complements traditional morphological analysis of fossil assemblages. *Quat. Sci. Rev.* **128**, 37–47 (2015).
12. Grealy, A. *et al.* Tropical ancient DNA from bulk archaeological fish bone reveals the subsistence practices of a historic coastal community in southwest Madagascar. *J. Archaeol. Sci.* **75**, 82–88 (2016).
13. Murray, D. C. *et al.* Scrapheap challenge: a novel bulk-bone metabarcoding method to investigate ancient DNA in faunal assemblages. *Sci. Rep.* **3**, 3371 (2013).

14. Haile, J. *et al.* Ancient DNA reveals late survival of mammoth and horse in interior Alaska. *Proc. Natl. Acad. Sci. USA* **106**, 22352–22357 (2009).
15. Pedersen, M. W. *et al.* Ancient and modern environmental DNA. *Philos. Trans. R. Soc. Lond. B Biol. Sci.* **370**, 20130383 (2015).
16. Pedersen, M. W. *et al.* Postglacial viability and colonization in North America's ice-free corridor. *Nature* **537**, 45–49 (2016).
17. Slon, V. *et al.* Neandertal and Denisovan DNA from Pleistocene sediments. *Science* **356**, 605–608 (2017).
18. Kistler, L., Ware, R., Smith, O., Collins, M. & Allaby, R. G. A new model for ancient DNA decay based on paleogenomic metaanalysis. *Nucleic Acids Res.* **45**, 6310–6320 (2017).
19. Allentoft, M. E. *et al.* The half-life of DNA in bone: measuring decay kinetics in 158 dated fossils. *Proceedings of the Royal Society B* **279**, 4724–4733 (2012).
20. Welker, F. *et al.* Ancient proteins resolve the evolutionary history of Darwin's South American ungulates. *Nature* **522**, 81–84 (2015).
21. Buckley, M., Collins, M. J., Thomas-Oates, J. & Wilson, J. C. Species identification by analysis of bone collagen using matrix-assisted laser desorption/ionisation time-of-flight mass spectrometry. *Rapid Commun. Mass Spectrom.* **23**, 3843–3854 (2009).
22. Buckley, M., Larkin, N. & Collins, M. Mammoth and Mastodon collagen sequences; survival and utility. *Geochim. Cosmochim. Acta* **75**, 2007–2016 (2011).
23. Cappellini, E. *et al.* Proteomic analysis of a pleistocene mammoth femur reveals more than one hundred ancient bone proteins. *J. Proteome Res.* **11**, 917–926 (2012).
24. Welker, F. Palaeoproteomics for human evolution studies. *Quat. Sci. Rev.* **190**, 137–147 (2018).
25. Brandt, L. Ø., Haase, K. & Collins, M. J. Species identification using ZooMS, with reference to the exploitation of animal resources in the medieval town of Odense. *Danish Journal of Archaeology* 1–15 (2018).
26. Evans, S. *et al.* Using combined biomolecular methods to explore whale exploitation and social aggregation in hunter–gatherer–fisher society in Tierra del Fuego. *Journal of Archaeological Science: Reports* **6**, 757–767 (2016).
27. von Holstein, I. C. C. *et al.* Searching for Scandinavians in pre-Viking Scotland: molecular fingerprinting of Early Medieval combs. *J. Archaeol. Sci.* **41**, 1–6 (2014).
28. Coutu, A. N., Whitelaw, G., le Roux, P. & Sealy, J. Earliest Evidence for the Ivory Trade in Southern Africa: Isotopic and ZooMS Analysis of Seventh–Tenth Century ad Ivory from KwaZulu-Natal. *Afr Archaeol Rev* 1–25 (2016).
29. Welker, F., Soressi, M., Rendu, W., Hublin, J.-J. & Collins, M. J. Using ZooMS to identify fragmentary bone from the late Middle/ Early Upper Palaeolithic sequence of Les Cottés, France. *J. Archaeol. Sci.* **54**, 279–286 (2015).
30. Welker, F. *et al.* Palaeoproteomic evidence identifies archaic hominins associated with the Châtelperronian at the Grotte du Renne. *Proc. Natl. Acad. Sci. USA* **113**, 11162–11167 (2016).
31. Devière, T. *et al.* Direct dating of Neanderthal remains from the site of Vindija Cave and implications for the Middle to Upper Paleolithic transition. *Proc. Natl. Acad. Sci. USA* **114**, 10606–10611 (2017).
32. Brown, S. *et al.* Identification of a new hominin bone from Denisova Cave, Siberia using collagen fingerprinting and mitochondrial DNA analysis. *Sci. Rep.* **6**, 23559 (2016).
33. Charlton, S., Alexander, M., Collins, M. & Milner, N. Finding Britain's last hunter-gatherers: A new biomolecular approach to 'unidentifiable' bone fragments utilising bone collagen. *Journal of Archaeological Science* **73**, 55–61 (2016).
34. Posth, C. *et al.* Deeply divergent archaic mitochondrial genome provides lower time boundary for African gene flow into Neanderthals. *Nat. Commun.* **8**, 16046 (2017).

35. Talamo, S. *et al.* Direct radiocarbon dating and genetic analyses on the purported Neanderthal mandible from the Monti Lessini (Italy). *Sci. Rep.* **6**, 29144 (2016).
36. Fellows Yates, J. A. *et al.* Central European Woolly Mammoth Population Dynamics: Insights from Late Pleistocene Mitochondrial Genomes. *Sci. Rep.* **7**, 17714 (2017).
37. Harvey, V. L., Egerton, V. M., Chamberlain, A. T., Manning, P. L. & Buckley, M. Collagen Fingerprinting: A New Screening Technique for Radiocarbon Dating Ancient Bone. *PLoS One* **11**, e0150650 (2016).
38. Welker, F. *et al.* Variations in glutamine deamidation for a Châtelperronian bone assemblage as measured by peptide mass fingerprinting of collagen. *STAR: Science & Technology of Archaeological Research* **3**, 15–27 (2017).
39. Simpson, J. P. *et al.* The effects of demineralisation and sampling point variability on the measurement of glutamine deamidation in type I collagen extracted from bone. *J. Archaeol. Sci.* **69**, 29–38 (2016).
40. van Doorn, N. L., Hollund, H. & Collins, M. J. A novel and non-destructive approach for ZooMS analysis: ammonium bicarbonate buffer extraction. *Archaeol. Anthropol. Sci.* **3**, 281–289 (2011).
41. Buckley, M., Harvey, V. L. & Chamberlain, A. T. Species identification and decay assessment of Late Pleistocene fragmentary vertebrate remains from Pin Hole Cave (Creswell Crags, UK) using collagen fingerprinting. *Boreas* **46**, 402–411 (2017).
42. Peresani, M., Bertola, S., Delpiano, D., Benazzi, S. & Romandini, M. The Uluzzian in the north of Italy: insights around the new evidence at Riparo Broion. *Archaeol. Anthropol. Sci.* **11**, 3503–3536 (2019).
43. Tagliacozzo, A., Romandini, M., Fiore, I., Gala, M. & Peresani, M. Animal Exploitation Strategies during the Uluzzian at Grotta di Fumane (Verona, Italy). In *Zooarchaeology and Modern Human Origins: Human Hunting Behavior during the Later Pleistocene* (eds Clark, J. L. & Speth, J. D.) 129–150 (Springer Netherlands, 2013).
44. Douka, K. *et al.* On the chronology of the Uluzzian. *J. Hum. Evol.* **68**, 1–13 (2014).
45. Peresani, M. Fifty thousand years of flint knapping and tool shaping across the Mousterian and Uluzzian sequence of Fumane cave. *Quat. Int.* **247**, 125–150 (2012).
46. Peresani, M., Cristiani, E. & Romandini, M. The Uluzzian technology of Grotta di Fumane and its implication for reconstructing cultural dynamics in the Middle–Upper Palaeolithic transition of Western Eurasia. *J. Hum. Evol.* **91**, 36–56 (2016).
47. Peresani, M. *et al.* Age of the final Middle Palaeolithic and Uluzzian levels at Fumane Cave, Northern Italy, using ¹⁴C, ESR, ²³⁴U/²³⁰Th and thermoluminescence methods. *J. Archaeol. Sci.* **35**, 2986–2996 (2008).
48. Falcucci, A., Conard, N. J. & Peresani, M. A critical assessment of the Protoaurignacian lithic technology at Fumane Cave and its implications for the definition of the earliest Aurignacian. *PLoS One* **12**, e0189241 (2017).
49. Broglio, A. *et al.* La production lamellaire et les armatures lamellaires de l'aurignacien ancien de la Grotte de Fumane (Monts Lessini, Vénétie). *Archéologiques* **1**, 415–436 (2005).
50. Broglio, A. *et al.* L'art aurignacien dans la décoration de la Grotte de Fumane. *Anthropologie* **113**, 753–761 (2009).
51. Peresani, M., Fiore, I., Gala, M., Romandini, M. & Tagliacozzo, A. Late Neandertals and the intentional removal of feathers as evidenced from bird bone taphonomy at Fumane Cave 44 ky BP, Italy. *Proc. Natl. Acad. Sci. USA* **108**, 3888–3893 (2011).
52. Peresani, M., Vanhaeren, M., Quaggiotto, E., Queffelec, A. & d'Errico, F. An ochered fossil marine shell from the mousterian of fumane cave, Italy. *PLoS One* **8**, e68572 (2013).
53. Romandini, M. *et al.* Neanderthal scraping and manual handling of raptors wing bones: Evidence from Fumane Cave. Experimental activities and comparison. *Quat. Int.* **421**, 154–172 (2016).
54. Martini, M., Sibilila, E., Croci, S. & Cremaschi, M. Thermoluminescence (TL) dating of burnt flints: problems, perspectives and some examples of application. *J. Cult. Herit.* **2**, 179–190 (2001).

55. López-García, J. M., dalla Valle, C., Cremaschi, M. & Peresani, M. Reconstruction of the Neanderthal and Modern Human landscape and climate from the Fumane cave sequence (Verona, Italy) using small-mammal assemblages. *Quat. Sci. Rev.* **128**, 1–13 (2015).
56. Higham, T. *et al.* Problems with radiocarbon dating the Middle to Upper Palaeolithic transition in Italy. *Quat. Sci. Rev.* **28**, 1257–1267 (2009).
57. Higham, T. European Middle and Upper Palaeolithic radiocarbon dates are often older than they look: problems with previous dates and some remedies. *Antiquity* **85**, 235–249 (2011).
58. Fiore, I., Gala, M. & Tagliacozzo, A. Ecology and subsistence strategies in the eastern Italian Alps during the Middle Palaeolithic. *Int. J. Osteoarchaeol.* **14**, 273–286 (2004).
59. Romandini, M., Nannini, N., Tagliacozzo, A. & Peresani, M. The ungulate assemblage from layer A9 at Grotta di Fumane, Italy: A zooarchaeological contribution to the reconstruction of Neanderthal ecology. *Quat. Int.* **337**, 11–27 (2014).
60. Terlato, G., Livraghi, A., Romandini, M. & Peresani, M. Large bovids on the Neanderthal menu: Exploitation of *Bison priscus* and *Bos primigenius* in northeastern Italy. *Journal of Archaeological Science: Reports* **25**, 129–143 (2019).
61. Binford, L. R. *Bones: ancient men and modern myths* (Academic Press, 1981).
62. Brain, C. K. *The hunters or the hunted?* (University of Chicago Press, 1981).
63. Potts, R. & Shipman, P. Cutmarks made by stone tools on bones from Olduvai Gorge, Tanzania. *Nature* **291**, 577 (1981).
64. Shipman, P. *Life history of a fossil: an introduction to taphonomy and paleoecology.* (Harvard University Press, 1981).
65. Shipman, P. & Rose, J. J. Cutmark Mimics on Modern and Fossil Bovid Bones. *Curr. Anthropol.* **25**, 116–117 (1984).
66. Blumenshine, R. J. Percussion marks, tooth marks, and experimental determinations of the timing of hominid and carnivore access to long bones at FLK Zinjanthropus, Olduvai Gorge, Tanzania. *J. Hum. Evol.* **29**, 21–51 (1995).
67. Lyman, R. L. *Vertebrate taphonomy.* (Cambridge University Press, 1994).
68. Fisher, J. W. Bone surface modifications in zooarchaeology. *J Archaeol Method Theory* **2**, 7–68 (1995).
69. Stiner, M. C., Kuhn, S. L., Weiner, S. & Bar-Yosef, O. Differential Burning, Recrystallization, and Fragmentation of Archaeological Bone. *J. Archaeol. Sci.* **22**, 223–237 (1995).
70. Grayson, D. K. *Quantitative Zooarchaeology* (Academic Press, 1984).
71. Wilson, J., van Doorn, N. L. & Collins, M. J. Assessing the extent of bone degradation using glutamine deamidation in collagen. *Anal. Chem.* **84**, 9041–9048 (2012).
72. van Doorn, N. L., Wilson, J., Hollund, H., Soressi, M. & Collins, M. J. Site-specific deamidation of glutamine: a new marker of bone collagen deterioration. *Rapid Commun. Mass Spectrom.* **26**, 2319–2327 (2012).
73. R Core Team. R: A Language and Environment for Statistical Computing. (R Foundation for Statistical Computing, 2018).
74. Wickham, H. *ggplot2: Elegant Graphics for Data Analysis* (Springer-Verlag New York, 2016).
75. Outram, A. K. A New Approach to Identifying Bone Marrow and Grease Exploitation: Why the ‘Indeterminate’ Fragments should not be Ignored. *J. Archaeol. Sci.* **28**, 401–410 (2001).
76. Welker, F. *et al.* Middle Pleistocene protein sequences from the rhinoceros genus *Stephanorhinus* and the phylogeny of extant and extinct Middle/Late Pleistocene Rhinocerotidae. *PeerJ* **5**, e3033 (2017).
77. Cleland, T. P., Schroeter, E. R., Feranec, R. S. & Vashishth, D. Peptide sequences from the first *Castoroides ohioensis* skull and the utility of old museum collections for palaeoproteomics. *Proc. Biol. Sci.* **283** (2016).
78. Tomasso, A. *et al.* Gravettian weaponry: 23,500-year-old evidence of a composite barbed point from Les Prés de Laure (France). *J. Archaeol. Sci.* **100**, 158–175 (2018).
79. Hublin, J.-J. The modern human colonization of western Eurasia: when and where? *Quat. Sci. Rev.* **118**, 194–210 (2015).

80. Moroni, A., Boscato, P. & Ronchitelli, A. What roots for the Uluzzian? Modern behaviour in Central-Southern Italy and hypotheses on AMH dispersal routes. *Quat. Int.* **316**, 27–44 (2013).
81. Palma di Cesnola, A. L'Uluzzien: Faciès italien du leptolithique archaïque. *Anthropologie* **93**, 783–811 (1989).
82. Peresani, M. L'Uluzzien en Italie. In *Néandertal/Cro-Magnon, La rencontre* (ed. Edition Errance, A.) 61–80 (Otte M., 2014).
83. Benazzi, S. *et al.* Early dispersal of modern humans in Europe and implications for Neanderthal behaviour. *Nature* **479**, 525–528 (2011).
84. Zilhão, J., Banks, W. E., d'Errico, F. & Gioia, P. Analysis of Site Formation and Assemblage Integrity Does Not Support Attribution of the Uluzzian to Modern Humans at Grotta del Cavallo. *PLoS One* **10**, e0131181 (2015).
85. Moroni, A., Ronchitelli, A., Arrighi, S. & Aureli, D. Grotta del Cavallo (Apulia–Southern Italy). The Uluzzian in the mirror. *Journal of Anthropological Sciences* **96**, 125–160 (2018).
86. Benazzi, S. *et al.* Middle Paleolithic and Uluzzian human remains from Fumane Cave, Italy. *J. Hum. Evol.* **70**, 61–68 (2014).
87. Benazzi, S. *et al.* The makers of the Protoaurignacian and implications for Neanderthal extinction. *Science* **348**, 793–796 (2015).
88. Morin, E. *Reassessing Paleolithic Subsistence: The Neanderthal and Modern Human Foragers of Saint-Césaire* (Cambridge University Press, 2012).
89. Ruebens, K., McPherron, S. J. P. & Hublin, J.-J. On the local Mousterian origin of the Châtelperronian: Integrating typo-technological, chronostratigraphic and contextual data. *J. Hum. Evol.* **86**, 55–91 (2015).
90. Stiner, M. C. Modern Human Origins Faunal Perspectives. *Annu. Rev. Anthropol.* **22**, 55–82 (1993).
91. Morin, E. Evidence for declines in human population densities during the early Upper Paleolithic in western Europe. *Proc. Natl. Acad. Sci. USA* **105**, 48–53 (2008).
92. Villa, P., Castel, J.-C., Beauval, C., Bourdillat, V. & Goldberg, P. Human and carnivore sites in the European Middle and Upper Paleolithic: similarities and differences in bone modification and fragmentation. *Revue de paléobiologie* **23**, 705–730 (2004).
93. Marín-Monfort, P. & Fernández-Jalvo, Y. Compressive marks from gravel substrate on vertebrate remains: a preliminary experimental study. *Quat. Int.* **330**, 118–125 (2014).
94. Fernández-Jalvo, Y., Andrews, P., Fernández-Jalvo, Y. & Andrews, P. Experimental effects of water abrasion on bone fragments. *Journal of Taphonomy* **1**, 147–163 (2003).
95. Blasco, R., Rosell, J., Fernández Peris, J., Cáceres, I. & Vergès, J. M. A new element of trampling: an experimental application on the Level XII faunal record of Bolomor Cave (Valencia, Spain). *J. Archaeol. Sci.* **35**, 1605–1618 (2008).
96. Stopp, M. Early Human Adaptation in the Northern Hemisphere and the Implications of Taphonomy. **669** (BAR International Series, 1997).
97. Isaac, G. L. Bones in contention: Competing explanations for the Juxtaposition of Early Pleistocene artefacts and faunal remains. In *Animals and Archaeology 1: Hunters and their Prey* (eds Clutton-Brock, J. & Grigson, C.) **163**, 3–19 (BAR International Series, 1983).
98. Smith, G. M. Taphonomic resolution and hominin subsistence behaviour in the Lower Palaeolithic: differing data scales and interpretive frameworks at Boxgrove and Swanscombe (UK). *J. Archaeol. Sci.* **40**, 3754–3767 (2013).
99. Fernández-Jalvo, Y. & Andrews, P. *Atlas of Taphonomic Identifications: 1001+ Images of Fossil and Recent Mammal Bone Modification* (Springer, Dordrecht, 2016).
100. García-Moreno, A., Smith, G. M., Kindler, L. & Pop, E. Evaluating the incidence of hydrological processes during site formation through orientation analysis. A case study of the middle Palaeolithic Lakeland site of Neumarkt-Nord 2 (Germany). *J. Archaeol. Sci.* **6**, 82–93 (2016).

101. Rabinovich, R., Gaudzinski-Windheuser, S., Kindler, L. & Goren-Inbar, N. The Acheulian site of Gesher Benot Ya'aqov Volume III: Mammalian Taphonomy. The assemblages of Layers V-5 and V-6. (Springer, Dordrecht, 2012).
102. James, E. C. & Thompson, J. C. On bad terms: Problems and solutions within zooarchaeological bone surface modification studies. *Environ. Archaeol.* **20**, 89–103 (2015).
103. Stiner, M. C. An Unshakable Middle Paleolithic?: Trends versus Conservatism in the Predatory Niche and Their Social Ramifications. *Curr. Anthropol.* **54**, S288–S304 (2013).
104. Gaudzinski, S. & Turner, E. The role of early humans in the accumulation of European Lower and Middle Palaeolithic bone assemblages. (Römisch-Germischen Zentralmuseums Mainz, 1999).
105. Gaudzinski, S. & Turner, E. The role of Hominins in the accumulation of Lower and Middle Palaeolithic bone assemblages. *Curr. Anthropol.* **37**, 153–156 (1996).
106. Gaudzinski, S. Subsistence patterns of Early Pleistocene hominids in the Levant—taphonomic evidence from the 'Ubeidiya Formation (Israel). *J. Archaeol. Sci.* **31**, 65–75 (2004).
107. Kindler, L., Smith, G. M. & Wagner, M. Initial assessment of the Neumark-Nord 2 fauna. In *Multidisciplinary studies of the Middle Palaeolithic record from Neumark-Nord (Germany) Volume 1. Veröffentlichungen des Landesamtes für Denkmalpflege und Archäologie 68* (eds Gaudzinski-Windheuser, S. & Roebroeks, W.) 197–211 (Landesamtes für Denkmalpflege und Archäologie Sachsen-Anhalt, Halle, 2014).
108. Gaudzinski-Windheuser, S. & Kindler, L. Research perspectives for the study of Neandertal subsistence strategies based on the analysis of archaeozoological assemblages. *Quat. Int.* **247**, 59–68 (2012).
109. Pickering, T. R., Marean, C. W. & Dominguez-Rodrigo, M. Importance of limb bone shaft fragments in zooarchaeology: a response to 'On *in situ* attrition and vertebrate body part profiles' (2002), by M.C. Stiner. *J. Archaeol. Sci.* **30**, 1469 (2003).
110. Bartram, J. L. E. & Marean, C. W. Explaining the 'Klasies Pattern': Kua Ethnoarchaeology, the Die Kelders Middle Stone Age Archaeofauna, Long Bone Fragmentation and Carnivore Ravaging. *J. Archaeol. Sci.* **26**, 9 (1999).
111. Lam, Y. M., Chen, X., Marean, C. W. & Frey, C. J. Bone Density and Long Bone Representation in Archaeological Faunas: Comparing Results from CT and Photon Densitometry. *J. Archaeol. Sci.* **25**, 559 (1998).
112. Morin, E., Speth, J. D. & Lee-Thorp, J. Middle Palaeolithic Diets. In *The Oxford Handbook of the Archaeology of Diet* (Oxford University Press, 2015).
113. Marean, C. W. & Assefa, Z. Zooarchaeological evidence for the faunal exploitation behaviour of Neanderthals and Early Modern Humans. *Evol. Anthropol.* **8**, 22–37 (1999).
114. Dusseldorp, G. L. A View to a Kill: Investigating Middle Palaeolithic Subsistence Using an Optimal Foraging Perspective. (Sidestone Press, 2009).
115. Cassoli, P. F. & Tagliacozzo, A. Considerazioni paleontologiche, paleoecologiche e archeozoologiche sui macromammiferi e gli uccelli dei livelli del Pleistocene superiore del Riparo di Fumane (VR) scavi 1988–91. *Boll. Mus. Civ. Stor. Nat. Verona* **18**, 349–445 (1991).

Acknowledgements

Research at Fumane is coordinated by the Ferrara University (MP) in the framework of a project supported by the Ministry of Culture – Veneto Archaeological Superintendence, public institutions (Lessinia Mountain Community - Regional Natural Park, Fumane Municipality), Foundations (Leakey Foundation, Spring 2015 Grant), and private associations and companies. The authors thank the Max Planck Society for making this research possible.

Shannon McPherron, Karen Ruebens, and Adeline Le Cabec are thanked for comments on previous versions. V.S.M. and G.M.S. are funded by the Max Planck Society. F.W. is supported by a Marie Skłodowska-Curie Action postdoctoral Fellowship awarded by the European Union (#795569) and a Leakey Foundation Autumn 2017 Grant. We would like to thank the editor Alex Mackay and four anonymous reviewers for their valuable comments and feedback that helped to improve the paper.

Author contributions

V.S.M., F.W. and G.M.S. designed the research. V.S.M. and F.W. performed the proteomic analysis. M.R. and M.P. performed zooarchaeological analysis. J.J.-H. and A.W. provided technical support. V.S.M., F.W. and G.M.S. wrote the manuscript with contributions of all authors.*

Additional information

Supplementary information accompanies this paper at <https://doi.org/10.1038/s41598-019-48706-z>.

SUPPLEMENTARY INFORMATION TO:

Combining ZooMS and zooarchaeology to study Late Pleistocene hominin behaviour at Fumane (Italy).

Virginie Sinet-Mathiot¹, Geoff M. Smith¹, Matteo Romandini^{2,3}, Arndt Wilcke⁴, Marco Peresani³, Jean-Jacques Hublin¹, Frido Welker^{1,5}

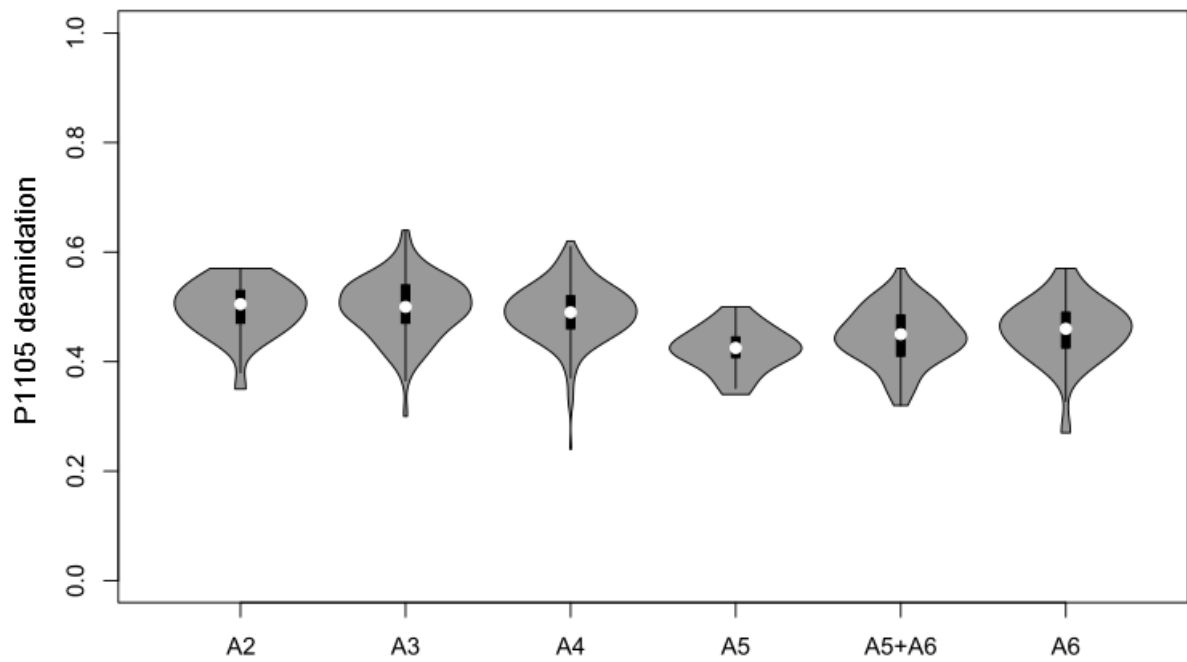
¹ Department of Human Evolution, Max Planck Institute for Evolutionary Anthropology, Leipzig, Germany.

² University of Bologna, Department of Cultural Heritage, Ravenna, Italy.

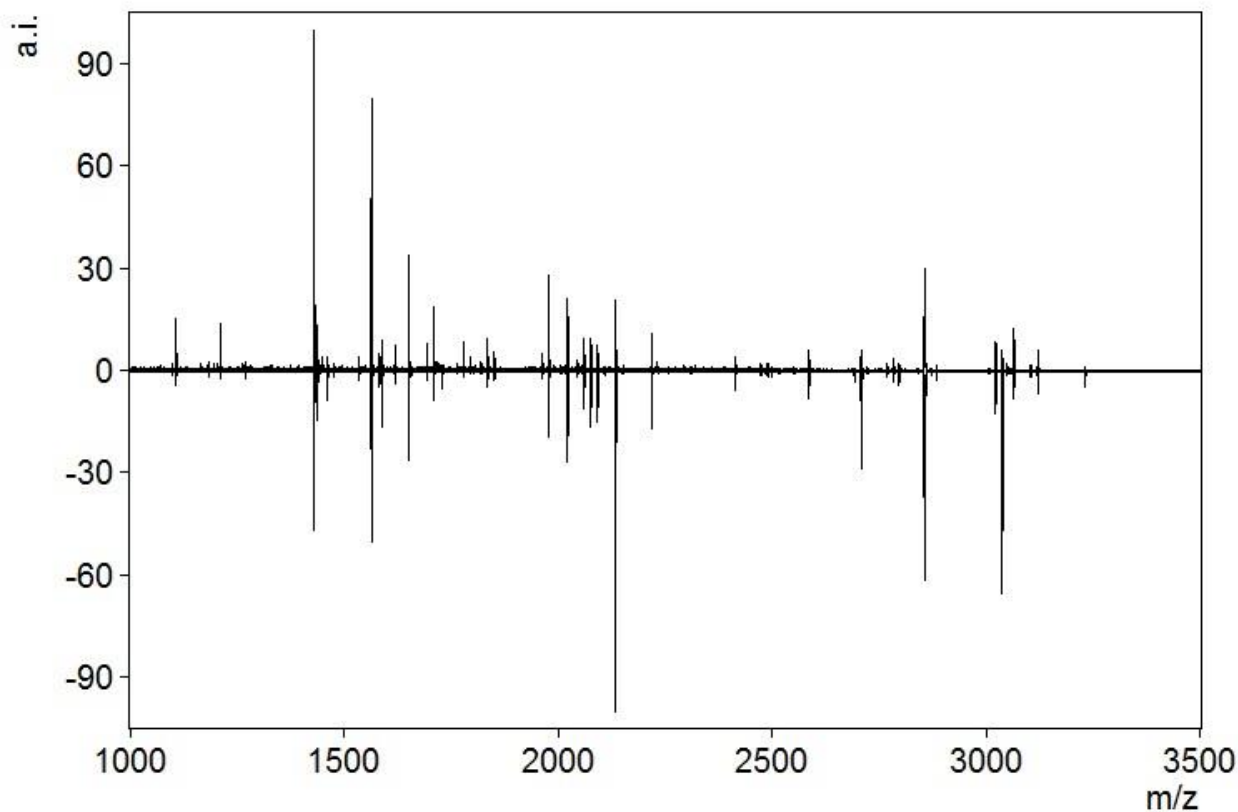
³ University of Ferrara, Department of Humanities, Section of Prehistory and Anthropology, Ferrara, Italy.

⁴ Fraunhofer Institute for Cell Therapy and Immunology, Leipzig, Germany

⁵ Section for Evolutionary Genomics, the Globe Institute, University of Copenhagen, Copenhagen, Denmark.



Supplementary Figure S1. Temporal cline of bone P1105 deamidation values across the Fumane stratigraphy. Chronologically younger layers (from A2) are less deamidated than chronologically older layers (to A6). P1105 deamidation distributions between different archaeological layers are significantly different at $p < 0.05$ for all comparisons except between the layers A3 (Uluzzian) and A4 (Final Mousterian; see main text).



Supplementary Figure S2. Comparison of an AmBic (top) and Acid (bottom) extract analysed in York and Leipzig, respectively. Spectra are displayed in the m/z range of 1000-3500, and concern the same morphologically unidentifiable bone specimen (F-258; Bos/Bison). Y-axis (top) and inverted y-axis (bottom) shows relative intensity to the highest peak in either spectrum.

Supplementary Table S1. Percentage of number of identified specimens (%NISP) of herbivores for the morphologically identified (Morph.) and the ZooMS-component (ZooMS) from Les Cottés (France), Quinçay (France), Pin Hole Cave (UK), and Grotte du Renne (France). Note that the values for Pin Hole are estimates as the original publication does not provide numeric information, only graphical.

Species	Les Cottés ZooMS	Les Cottés Morph .	Quincay ZooMS	Quincay Morph.	Pin Hole ZooMS	Pin Hole Morph.	Grotte du Renne ZooMS	Grotte du Renne Morph.
<i>Bos/Bison</i>	32.9	26.7	21.1	13.6	7.0	6.8	5.6	4.0
<i>Capra</i> sp.	1.4	0	0	0	0	0	0.9	0
Ovis-type	0	0	0.7	1.4	0	0	0	0
Cervid/Saiga	5.7	0	1.0	2.8	2.1	0	10.2	0
<i>Capreolus capreolus</i>	0	0	0	0	0	0	0	0
<i>Rangifer tarandus</i>	32.9	54.7	33.7	42.2	60.5	62.0	45.4	55.0
Suidae	1.4	0	1.0	0	0	0	0	0
Equidae	18.6	14.7	39.8	35.2	9.2	9.3	26.9	20.0
Elephantidae	2.9	4.0	1.2	0.9	5.2	5.3	7.4	21.0
Rhinocerotidae	4.3	0	1.5	3.8	16.0	16.5	3.7	0

Supplementary Table S2. Squares, sublayers and layers studied with ZooMS. For further information see Peresani et al. ^{44,81,92}.

Layers	Sublayers	Squares
A2	A2R; A2+A2R	116; 117; 127; 128
A3	A3; A3I; A3II; A3III; A3IV; A3-A4II; A3 tetto;	56; 57; 58; 59; 66; 67; 68; 69; 76; 77; 78; 79; 86; 87; 88; 89; 97; 98
A4	A4; A4II; A4II/A5-A6; A4IV; A4V; A4V/A5-A6; A4V/A5; A4VI; A4VI/A5A6; A4-A5	56; 57; 58; 59; 66; 67; 68; 69; 76; 77; 78; 79; 86; 87; 88; 89; 96; 97; 98; 99; 106; 107; 108; 109; 116; 117; 118
A5	A5	41; 53; 61; 62; 71; 72
A5+A6	A5+A6; A5+A6-A6	60; 65; 70; 75; 81; 90; 91; 95; 100; 101; 105; 106; 107; 108; 111; 116; 117; 118
A6	A6	51; 61; 80; 117; 118

Supplementary Table S3. ZooMS species IDs for all studied levels. Percentages in the bottom row indicate the identification success rate per level. In the context of Fumane, Cervid/Saiga can be attributed to either *Cervus elaphus* (red deer), *Megaloceros giganteus* (giant deer) or *Alces alces* (elk), as an attribution to *Saiga* sp. or *Dama* sp. can be excluded based on our knowledge of the fauna in this region for this period. Ovis-type includes non-*Capra* sp. members of the Caprinae. In the context of Fumane an attribution to *Rupicapra rupicapra* (chamois) is possible. Canidae includes members of *Canis* sp. and *Vulpes alopex* (arctic fox), both of which are known morphologically at Fumane, but based on the ZooMS marker series an attribution to *Vulpes vulpes* can be excluded. Felinae is represented morphologically by *Lynx lynx* at the site for the stratigraphic portion considered in this study, and is the most likely species candidate for this taxonomic group in the ZooMS component.

Species	A2	A3	A4	A5	A5+A6	A6
Canidae (not red fox)	0	1	4	0	0	0
Red fox	0	1	3	0	0	0
Felinae	0	2	1	0	0	0
Ursidae	0	0	7	0	5	1
<i>Bos/Bison</i>	7	88	76	1	7	1
<i>Capra</i> sp.	5	23	12	0	8	1
Ovis-type	1	13	21	2	3	1
Cervid/Saiga	11	80	141	15	86	22
<i>Capreolus</i> sp.	0	8	3	1	2	0
Rhinocerotidae	0	1	1	0	0	0
Elephantidae	0	0	3	0	0	0
Pantherinae/Hyaenidae	0	1	0	0	0	0
Cervidae/Bovidae	0	1	0	0	0	0
Cervid/Saiga/Roe deer	0	3	3	1	0	0
Indeterminate	0	0	2	0	4	0
Total	24 (100%)	222 (98%)	277 (98%)	20 (95%)	115 (97%)	26 (100%)

Supplementary Table S4. A3 and A4 surface modification frequencies for the three main species groups per identification method. All agents of surface modification presented in the table below relate to the frequency of presence for each of these attributes. Data for all studied squares for both ZooMS and morphological analysis are included. Dental remains and burned specimens are not included in the calculation of the shown percentages. See Supplementary Table S5 for similar frequencies derived from a restricted set of squares. Numbers listed are percentages of occurrence and those in parentheses are number of specimens. ZooMS: bone component identified through ZooMS analysis. Morph.: bone component identified through morphology.

		Cervid/Saiga		Capra sp.		Bos/Bison	
		ZooMS	Morph.	ZooMS	Morph.	ZooMS	Morph.
Weathering	A3	27.4 (14)	15.6 (25)	21.4 (3)	15.6 (13)	20.7 (11)	40.0 (8)
	A4	43.0 (40)	21.9 (40)	25.0 (1)	24.0 (12)	15.5 (7)	52.9 (9)
Concretion	A3	33.3 (17)	26.8 (43)	14.2 (2)	32.5 (27)	24.5 (13)	60.0 (12)
	A4	20.4 (19)	39.0 (71)	50.0 (2)	22.0 (11)	17.7 (8)	52.9 (9)
Corrosion	A3	15.6 (8)	5.6 (9)	42.8 (6)	24.0 (20)	20.7 (11)	30.0 (6)
	A4	10.7 (10)	9.9 (18)	50.0 (2)	18.0 (9)	20.0 (9)	17.6 (3)
Exfoliation	A3	5.9 (3)	25.6 (41)	0.0 (0)	15.6 (13)	16.9 (9)	35.0 (7)
	A4	10.7 (10)	22.5 (41)	0.0 (0)	18.0 (9)	11.1 (5)	23.5 (4)
Mineral staining	A3	29.4 (15)	16.8 (27)	21.4 (3)	16.8 (14)	9.4 (5)	15.0 (3)
	A4	25.8 (24)	32.4 (59)	25.0 (1)	34.0 (17)	13.3 (6)	5.9 (1)
Root etching	A3	64.7 (33)	59.3 (95)	50.0 (7)	44.5 (37)	49.0 (26)	60.0 (12)
	A4	69.8 (65)	53.2 (97)	75.0 (3)	46.0 (23)	57.7 (26)	47.0 (8)
Carnivore and/or Rodent marks	A3	5.9 (3)	1.9 (3)	14.2 (2)	15.6 (13)	1.9 (1)	25.0 (5)
	A4	3.2 (3)	3.8 (7)	0.0 (0)	4.0 (2)	8.9 (4)	0.0 (0)
Cut marks	A3	58.8 (30)	36.8 (59)	35.7 (5)	24.0 (20)	32.0 (17)	50.0 (10)
	A4	44.0 (41)	48.9 (89)	25.0 (1)	16.0 (8)	13.3 (6)	41.1 (7)
Impact points	A3	7.8 (4)	21.8 (35)	7.14 (1)	4.81 (4)	15.0 (8)	10.0 (2)
	A4	13.9 (13)	19.7 (36)	0.0 (0)	6.0 (3)	24.4 (11)	35.2 (6)
Percussion Marks	A3	3.9 (2)	4.4 (7)	0.0 (0)	0.0 (0)	30.1 (16)	0.0 (0)
	A4	2.2 (2)	3.3 (6)	0.0 (0)	0.0 (0)	11.1 (5)	0.0 (0)

Total NISP	A3	51	160	14	83	53	20
	A4	93	182	4	50	45	17

Supplementary Table S5. A3 and A4 surface modification frequencies for the three main species groups per identification method, derived from the squares also covered by ZooMS sampling. All agents of surface modification presented in the table below relate to the frequency of presence for each of these attributes. Data for all studied squares for both ZooMS and morphological analysis are included. Dental remains and burned specimens are not included in the calculation of the shown percentages. Numbers listed are percentages of occurrence and those in parentheses are number of specimens. ZooMS: bone component identified through ZooMS analysis. Morph.: bone component identified through morphology.

		Cervid/Saiga		Capra sp.		Bos/Bison	
		ZooMS	Morph.	ZooMS	Morph.	ZooMS	Morph.
Weathering	A3	27.4 (14)	35.0 (7)	21.4 (3)	23.0 (3)	20.7 (11)	50.0 (3)
	A4	43.0 (40)	37.2 (19)	25.0 (1)	63.6 (7)	15.5 (7)	85.7 (6)
Concretion	A3	33.3 (17)	15.0 (3)	14.2 (2)	15.3 (2)	24.5 (13)	50.0 (3)
	A4	20.4 (19)	21.5 (11)	50.0 (2)	9.1 (1)	17.7 (8)	57.1 (4)
Corrosion	A3	15.6 (8)	20.0 (4)	42.8 (6)	38.4 (5)	20.7 (11)	33.3 (2)
	A4	10.7 (10)	11.7 (6)	50.0 (2)	27.2 (3)	20.0 (9)	14.2 (1)
Exfoliation	A3	5.88 (3)	15.0 (3)	0.0 (0)	7.7 (1)	16.9 (9)	16.6 (1)
	A4	10.7 (10)	25.4 (13)	0.0 (0)	9.1 (1)	11.1 (5)	28.5 (2)
Mineral staining	A3	29.4 (15)	15.0 (3)	21.4 (3)	7.7 (1)	9.4 (5)	0.0 (0)
	A4	25.8 (24)	47.0 (24)	25.0 (1)	27.2 (3)	13.3 (6)	0.0 (0)
Root etching	A3	64.7 (33)	65 (13)	50.0 (7)	61.5 (8)	49.0 (26)	50.0 (3)
	A4	69.8 (65)	43.1 (22)	75.0 (3)	45.4 (5)	57.7 (26)	57.1 (4)
Carnivore and/or rodent marks	A3	5.88 (3)	10.0 (2)	14.2 (2)	15.3 (2)	1.88 (1)	16.6 (1)
	A4	3.22 (3)	1.96 (1)	0.0 (0)	0.0 (0)	8.9 (4)	0.0 (0)
	A3	58.8 (30)	55.0 (11)	35.7 (5)	15.3 (2)	32.0 (17)	33.3 (2)

Cut marks	A4	44.0 (41)	52.9 (27)	25.0 (1)	18.1 (2)	13.3 (6)	71.4 (5)
Impact points	A3	7.8 (4)	15.0 (3)	7.1 (1)	7.7 (1)	15.0 (8)	33.3 (2)
	A4	13.9 (13)	19.6 (10)	0.0 (0)	27.2 (3)	24.4 (11)	57.1 (4)
Percussion Marks	A3	3.9 (2)	0.0 (0)	0.0 (0)	0.0 (0)	30.1 (16)	0.0 (0)
	A4	2.2 (2)	0.0 (0)	0.0 (0)	0.0 (0)	11.1 (5)	0.0 (0)
Total NISP	A3	51	20	14	13	53	6
	A4	93	51	4	11	45	7